THE JOURNAL OF BIOLOGICAL CHEMISTRY VOL. 290, NO. 2, pp. 1222–1232, January 9, 2015

Comparison of the Enzymatic and Functional Properties of Three Cytosolic Carboxypeptidase Family Members*

Received for publication, August 18, 2014, and in revised form, October 23, 2014 Published, JBC Papers in Press, November 21, 2014, DOI 10.1074/jbc.M114.604850

Hui-Yuan Wu[‡], Yongqi Rong[‡], Kristen Correia[‡], Jaeki Min[§], and James I. Morgan[‡1]

From the Departments of [‡]Developmental Neurobiology and [§]Chemical Biology and Therapeutics, St. Jude Children's Research Hospital, Memphis, Tennessee 38105

Background: All cytosolic carboxypeptidase (CCP) family members catalyze deglutamylation of tubulin.
Results: Nna1 (CCP1), CCP4, and CCP6 exhibit distinct sequence preferences and kinetics for synthetic polyglutamate substrates. CCP4 and CCP6 fail to rescue Purkinje cell degeneration in Nna1-dysfunctional mice.
Conclusion: CCPs are not biologically equivalent in Purkinje neurons.
Significance: The results expand the range of substrates and biological processes influenced by CCPs.

Nna1 (CCP1) defines a subfamily of M14 metallocarboxypeptidases (CCP1–6) and is mutated in *pcd* (Purkinje cell degeneration) mice. Nna1, CCP4, and CCP6 are involved in the post-translational process of polyglutamylation, where they catalyze the removal of polyglutamate side chains. However, it is unknown whether these three cytosolic carboxypeptidases share identical enzymatic properties and redundant biological functions. We show that like Nna1, purified recombinant CCP4 and CCP6 deglutamylate tubulin, but unlike Nna1, neither rescues Purkinje cell degeneration in *pcd* mice, indicating that they do not have identical functions. Using biotin-based synthetic substrates, we established that the three enzymes are distinguishable based upon individual preferences for glutamate chain length, the amino acid immediately adjacent to the glutamate chain, and whether their activity is enhanced by nearby acidic amino acids. Nna1 and CCP4 remove the C-terminal glutamate from substrates with two or more glutamates, whereas CCP6 requires four or more glutamates. CCP4 behaves as a promiscuous glutamase, with little preference for chain length or neighboring amino acid composition. Besides glutamate chain length dependence, Nna1 and CCP6 exhibit higher k_{cat}/K_m when substrates contain nearby acidic amino acids. All cytosolic carboxypeptidases exhibit a monoglutamase activity when aspartic acid precedes a single glutamate, which, together with their other individual preferences for flanking amino acids, greatly increases the potential substrates for these enzymes and the biological processes in which they act. Additionally, Nna1 metabolized substrates mimicking the C terminus of tubulin in a way suggesting that the tyrosinated form of tubulin will accumulate in *pcd* mice.

Nna1 is the prototype of a subfamily of M14 metallocarboxypeptidases (CCP1–6)[2] (1–3) that was first identified through its marked induction in axotomized spinal motor neurons (1). Subsequently, we showed that loss-of-function mutations of *Agtpbp1*, the gene encoding Nna1, underlie the *pcd* (Purkinje cell degeneration) mutant mouse (4), which exhibits selective degeneration of neurons in the cerebellum, thalamus, olfactory bulb, and retina (5). Recently, a recessive mutation in *Agtpbp1* was also shown to cause lower motor neuron degeneration in sheep (6). The realization that Nna1 is a potential link point between regenerative and degenerative processes in neurons spurred a search for its biological function.

Nna1 harbors a carboxypeptidase domain, and point mutations to critical residues in its predicted substrate-binding site (3, 7), zinc-binding motif (8), and catalytic center (7) destroy its biological activity *in vivo*, indicating that its catalytic activity is essential. In parallel, Nna1 and its related family members, CCP4–6, were demonstrated to be glutamases (9, 10), enzymes that catabolize runs of glutamic acid either at the C terminus of proteins or in covalently attached side chains that are added to some proteins (notably tubulin) through a post-translational process termed polyglutamylation (reviewed in Ref. 11). Polyglutamylation is a dynamic process in which glutamate residues are added to a branch point glutamate in the primary amino acid chain of substrate proteins by tubulin-tyrosine ligase-like (TTLL) enzymes and removed by the Nna1 subfamily of glutamases (7, 9, 10). These studies suggested that Nna1 functions in polyglutamylation by trimming polyglutamate chains and that disruption of this equilibrium in *pcd* mice leads to increased glutamate chain length on critical proteins such as tubulin and subsequent neurodegeneration (7, 10). However, other features of the *pcd* mouse suggest that the situation *in vivo* may be more complex.

Nna1 is widely expressed in the adult and developing mouse brain, yet only certain populations of neurons degenerate in adult *pcd* mice (5). We suggested that this might be a consequence of overlapping expression or redundancy with other

* This work was supported, in whole or in part, by National Institutes of Health Cancer Center Support Grant CA 21765 from NCI and Grant NS051537 (to J. I. M.). This work was also supported by the American Lebanese Syrian Associated Charities.

[1] To whom correspondence should be addressed: Department of Developmental Neurobiology, St. Jude Children's Research Hospital, 262 Danny Thomas Place, Memphis, TN 38105. Tel.: 901-595-2258; Fax: 901-595-3143; E-mail: jim.morgan@stjude.org.

[2] The abbreviations used are: CCP, cytosolic carboxypeptidase; TTLL, tubulin-tyrosine ligase-like; BisTris, 2-[bis(2-hydroxyethyl)amino]-2-(hydroxymethyl)propane-1,3-diol; Tg, transgene.

Nna1 subfamily members, such as CCP4 and CCP6 (3), that are reported to catalyze the identical glutamase reaction *in vitro* (10). The primary objectives of this study were to determine whether the three CCPs have identical enzymatic and functional properties and whether these properties are consistent with the enzymes contributing to the selective neurodegeneration in *pcd* mice. Here, we compared the enzymatic properties of purified recombinant Nna1, CCP4, and CCP6 and determined whether CCP4 or CCP6 can rescue Purkinje cell loss in *pcd* mice using an established transgenic mouse model (3, 7). We confirmed that Nna1, CCP4, and CCP6 all metabolize the polyglutamate side chains of tubulin. In addition, using synthetic substrates, we showed they have distinct kinetic properties and preferences for glutamate chain length and different requirements for acidic amino acids near the branch point glutamate. Moreover, whereas transgenic expression of Nna1 fully rescued Purkinje cell loss in *pcd* mice, CCP4 and CCP6 had little or no activity, indicating that they are not functionally equivalent to Nna1 *in vivo*.

EXPERIMENTAL PROCEDURES

Animals—pcd$^{3J+/-}$, FVB/NJ, and C57BL/6J mice were purchased from the Jackson Laboratory (Bar Harbor, ME). Animals were maintained on a 12-h light/12-h dark cycle with free access to food and water. All studies were approved by the St. Jude Children's Research Hospital Animal Care and Use Committee and complied with the standards set forth in the *National Institutes of Health Guide for the Care and Use of Laboratory Animals* (34).

Generation of CCP Transgenic Mice—Blunt-ended PCR products of the ORFs of mouse *CCP4* (FN429927) and *CCP6* (FN429928) were inserted into the unique BamHI site of the fourth exon of the *L7* gene in a pGEM-3 vector (12). The *L7-CCP* transgenes were subsequently released from the pGEM-3 vector using EcoRI and HindIII, purified, sequenced, and injected into the male pronucleus of fertilized oocytes as described previously (3, 7, 12). Offspring were genotyped for the presence of *L7-CCP4* transgenes using primers 5′-CTGACCAAATACCACCACCCT-3′ and 5′-GGTCACATCAAGCGCTTCTAAT-3′ and of the *L7-CCP6* transgenes using primers 5′-CTCAAAATAATCCTCCTGCCTG-3′ and 5′-CCGGCCTAATGAACAGATCATA-3′. Genotyping of the wild-type and *pcd^{3J}* alleles of *Nna1* was performed as described (4, 13). Three *L7-CCP4* and eight *L7-CCP6* transgenic lines were generated.

We characterized at least two independent lines for each construct. Subsequently, all lines of transgenic mice were crossed repeatedly with *pcd$^{3J+/-}$* mice to produce *pcd$^{3J-/-}$/Tg* mice and all intermediate genotypes.

RT-PCR Analysis of Transgenic Expression—Mouse cerebellums were snap-frozen in dry ice, and total RNA was extracted with TRIzol reagent (Invitrogen). The levels of *L7-CCP4* and *L7-CCP6* chimeric mRNAs in transgenic mice were monitored by RT-PCR. First-strand cDNA was generated by reverse transcription using the SuperScript III first-strand synthesis system (Invitrogen) according to the manufacturer's protocol. Primers 5′-CCCTGCTCCAGAGAAGGACA-3′ and 5′-GCTGAAGAGAGTCTCCATGCCT-3′ were used for *L7-CCP4* transgenic lines, and primers 5′-CCCTGCTCCAGAGAAGGACA-3′ and 5′-CCATCTCGGTAAAGACTCTTGG-3′ were used to evaluate expression of *L7-CCP6* mRNA in transgenic mice. As a loading control, β-actin was amplified using primers 5′-AGGATGGCGTGAGGGAGAGC-3′ and 5′-ATATCGCTGCGCTGGTCGTC-3′. Those lines with the highest levels of transcript of the desired transgene were chosen for further analysis.

Histology and Immunohistochemistry—The procedures for histological analyses of cerebellums were as described (3, 14). To visualize Purkinje cells, a rabbit anti-calbindin-D28K antibody (Sigma) was used at a dilution of 1:500, and immune complexes were revealed using a peroxidase-conjugated anti-rabbit kit and diaminobenzidine tetrahydrochloride substrate (Dako, Carpinteria, CA). After immunostaining, sections were counterstained with hematoxylin (Vector Labs, Burlingame, CA).

Preparation of Recombinant Mouse CCP4 and CCP6—Recombinant mouse CCP4 or CCP6 constructs containing a 6-histidine tag at their N termini were introduced into a baculovirus expression vector (pFastBac-HT-B) and used for large-scale protein production in insect cells in the Protein Production Facility at St. Jude Children's Research Hospital. The recombinant protein was purified to near homogeneity by nickel chelate chromatography. His-CCP4 was dialyzed to remove the imidazole after elution from the nickel column. Because of protein aggregation during dialysis, His-CCP6 was not subjected to dialysis. Protein purity was monitored by Coomassie Blue staining and immunoblotting.

Protein Electrophoresis and Immunoblotting—Recombinant CCPs were separated using a Criterion XT 4–12% BisTris precast gel (Bio-Rad). After electrophoresis, proteins were transferred onto a nitrocellulose membrane using the Criterion blotter (Bio-Rad). Membranes were incubated with mouse anti-polyglutamate (B3, 1:2000; Sigma), mouse anti-glutamate (GT335; Adipogen, San Diego, CA), or rabbit anti-α-tubulin (EP1332Y, 1:3000; Millipore) antibody. Immunoreactive protein bands were visualized with SuperSignal West Pico chemiluminescence substrate (Thermo Fisher Scientific, Rockford, IL) following incubation with HRP-labeled sheep anti-mouse (1:2000; Sigma) or donkey anti-rabbit (1:10,000; Sigma) antiserum.

Assay of CCP Carboxypeptidase Activity—All synthetic substrates tested were synthesized in the Hartwell Center for Bioinformatics and Biotechnology at St. Jude Children's Research Hospital. To examine the activity of recombinant CCPs on these synthetic substrates, a 500-μl reaction mixture comprising 3 μg of purified CCP, 100 mM NaCl, and 40 μM substrates in 25 mM HEPES-K buffer (pH 7.4) was incubated at 37 °C. Heat-denatured enzyme was incubated under identical conditions as a control. Reactions were terminated with 1 ml of ninhydrin-$CdCl_2$ reagent, and released amino acids were detected as described previously (Ref. 15, Method C) and quantified using a standard curve generated with known amounts of glutamic acid (Sigma).

Tubulin Glutamylase Assay—To determine CCP activity for the polyglutamate component of tubulin, a 20-μl reaction mixture containing 2 μg of CCP and 1 μg of porcine tubulin (Cytoskeleton, Inc., Denver, CO) in PBS was incubated at 37 °C. Reactions containing heat-denatured enzyme or intact enzyme in the presence of the metallocarboxypeptidase inhibitor 1,10-

phenanthroline (5 mM) (16, 17) served as controls of specificity. Reactions were terminated with 3× sample buffer. Samples were subsequently subjected to immunoblot analysis using antibody B3 (anti-polyglutamate), GT335 (anti-branch point glutamate), or EP1332Y (anti-α-tubulin).

Enzyme Kinetics—We previously described a synthetic substrate assay for measuring the enzymatic properties of Nna1 (7) and have extended this here to measure and compare the kinetics and substrate preferences of Nna1, CCP4, and CCP6. To determine the enzyme kinetics (K_m and V_{max}) and substrate preference of recombinant CCP4 (and Nna1), 50, 100, 200, 400, or 500 μM biotin-2E, biotin-3E, biotin-3EG2E, or biotin-2EG3E was incubated with 3 μg of enzyme in a 500-μl reaction containing 25 mM HEPES-K and 100 mM NaCl at 37 °C. To determine the enzyme kinetics of recombinant CCP6, 50, 100, 200, 320, of 500 μM biotin-3EG2E or biotin-2EG3E was incubated with 3 μg of CCP6 under the same conditions as for CCP4. Reactions were terminated after 15 min with ninhydrin-$CdCl_2$, and the initial rates of reaction were determined. Reactions were run in triplicate. Linear regression of the double-reciprocal plots of initial rates against substrate concentrations were generated using Microsoft Excel. The K_m and V_{max} values were calculated according to Mathews *et al.* (18).

LC-MS—Biotin-3EG2E (40 μM) was incubated with 3 μg of recombinant Nna1, CCP4, or CCP6 in a 500-μl reaction buffered with 25 mM HEPES-K in the presence of 100 mM NaCl at 37 °C. The reaction was terminated with an equal volume of methanol containing 0.2% formic acid. Samples (5 μl) were analyzed with an ACQUITY UPLC system and SQ detector (Waters, Milford, MA) equipped with a Waters ACQUITY UPLC BEH C18 column (2.1 × 50 mm, 1.7 μm). The column temperature was 40 °C, and the mobile phase was a gradient from 0 to 95% methanol in water with 0.05% formic acid for 2 min at a flow rate of 0.5 ml/min. The detection acquisition range was for ES+ scan from 500 to 1100 *m*/*z*.

Rotarod Test—Gender- and age-matched wild-type and $pcd^{3J-/-}$ littermate mice and $pcd^{3J-/-}$ littermate mice harboring either *L7-CCP4* or *L7-CCP6* transgenes were tested on an accelerating rotarod (San Diego Instruments, San Diego, CA) to assess motor coordination, balance, and motor learning. The rotarod was programmed to accelerate from 0 to 40 rpm in 4 min and then hold constant speed for an additional minute. The amount of time that elapsed before the mouse fell off was recorded. The maximum observation time was 5 min. Animals were given two trials per day with a 20-min intertrial interval. Animals were tested for 5 consecutive days. The latency of the mice to fall from the rod was scored as an index of their motor coordination. Improvement in performance across training days indicates motor learning (14, 19). The test data were expressed as the mean ± S.E. and were analyzed for statistical significance using one-way analysis of variance followed by Bonferroni's multiple comparison test or Student's *t* test depending on the case. The level of significance was set at $p < 0.05$.

Statistical Methods—Student's *t* test or one-way analysis of variance was used to compare independent samples for statistical significance. Significance was set at $p < 0.05$. Statistical analyses were performed using Microsoft Excel software.

RESULTS

Recombinant Nna1, CCP4, and CCP6 Metabolize the Polyglutamate Side Chain of Tubulin—Previous enzymatic studies of Nna1 family members were performed using tubulin as substrate and lysates of cells transfected with CCP4 and CCP6 as a source of enzyme with detection using an antibody to the polyglutamate chain of tubulin (10). As it is not practical to use this approach to determine details of enzyme kinetics or substrate preferences, we generated and purified N-terminally histidine-tagged versions of Nna1 (7) and CCP4 and CCP6 (Fig. 1*A*). When incubated with porcine brain tubulin, all three enzymes reduced B3 immunoreactivity in a time-dependent manner (Fig. 1*B*), which is indicative of removal of polyglutamate side chains (20, 21). Nna1 consistently showed the highest activity in this assay, with CCP4 and CCP6 being roughly equipotent (Fig. 1*B* and data not shown). The activity of all recombinant enzymes was abolished by treatment with the general metallocarboxypeptidase inhibitor 1,10-phenanthroline and by heat denaturation (Fig. 1*C*). These data confirm previous *in vitro* studies that Nna1, CCP4, and CCP6 all metabolize polyglutamate chains of tubulin (10, 22).

Nna1 Family Members Have Differential Preferences for Polyglutamate Chain Lengths—To characterize the kinetic properties of the recombinant enzymes, we utilized an assay in which we quantified glutamate release from biotin-based synthetic substrates containing glutamate chains of different length (7). Both recombinant Nna1 and CCP4 metabolized substrates with two or more glutamate residues (biotin-2E through biotin-5E) (Fig. 2*A*). In marked contrast, recombinant CCP6 had no activity on either biotin-2E or biotin-3E, whereas it did metabolize biotin-4E and biotin-5E (Fig. 2*A*), indicating a marked preference for longer glutamate chains and an inability to metabolize short glutamate chains. Although Nna1 could metabolize short glutamate chains, it was more active against longer chain substrates (Fig. 2*A*) (7), whereas CCP4 had no marked preference for chain length (Fig. 2, *A* and *B*). CCP6 was more like Nna1, showing a higher glutamate release rate from biotin-5E compared with biotin-4E (Fig. 2*C*).

It was surprising that CCP6 did not cleave substrates with fewer than four glutamate residues, as it did metabolize the polyglutamate chains of tubulin (Fig. 1*B*), where loss of B3 binding is thought to reflect degradation of chains to fewer than two glutamate residues (20, 21). Because polyglutamylation often occurs in a glutamate-rich region, we considered the possibility that the activity of CCP6 might be influenced by the amino acids flanking the polyglutamate chain. The best characterized substrate for polyglutamylation is tubulin (23–26). In α-tubulin, the branch point glutamate is preceded by a glycine and glutamate and followed by two additional glutamate residues (EG**E**EE, where the boldface *E* is the branch point glutamate). Therefore, we synthesized substrates that mimicked this region of α-tubulin (biotin-3EG2E and biotin-2EG3E) and compared them with biotin-2E and biotin-3E, respectively. CCP4 exhibited no particular preference for any of the substrates (Fig. 2*D*). In contrast, the presence of the flanking amino acids markedly enhanced the activities of both Nna1 and CCP6 compared with the respective glutamate-only substrates. Indeed, whereas

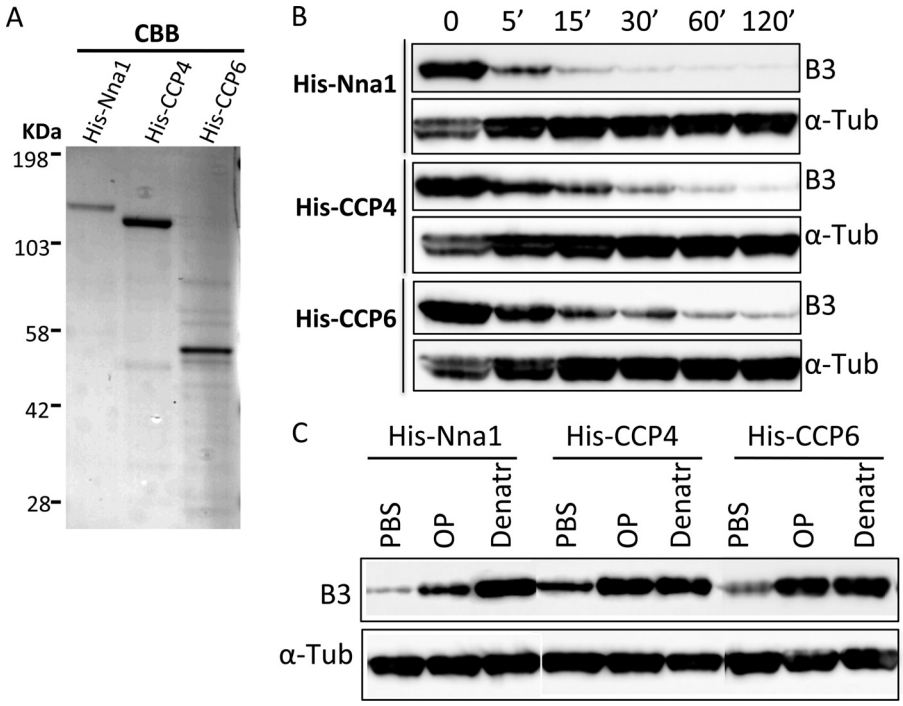

FIGURE 1. **Purified recombinant CCP4 and CCP6 catalyze the deglutamylation of porcine tubulin.** *A*, SDS-PAGE of purified recombinant Nna1, CCP4, and CCP6 stained with Coomassie Brilliant Blue (*CBB*). *B*, time courses of deglutamylation of porcine tubulin with recombinant Nna1, CCP4, and CCP6. Deglutamylation was monitored by immunoblotting using antibody B3. All three enzymes reduced the B3 signal (indicative of reduced polyglutamate chain length) of porcine tubulin in a time-dependent fashion, but with differing kinetics. *C*, the enzymatic activities of recombinant Nna1, CCP4, and CCP6 were inhibited by heat denaturation (*Denatr*) and 5 mM 1,10-phenanthroline (*OP*). To control for loading and integrity of tubulin during incubation with enzymes, α-tubulin (*α-Tub*) levels were monitored using antibody EP1332Y.

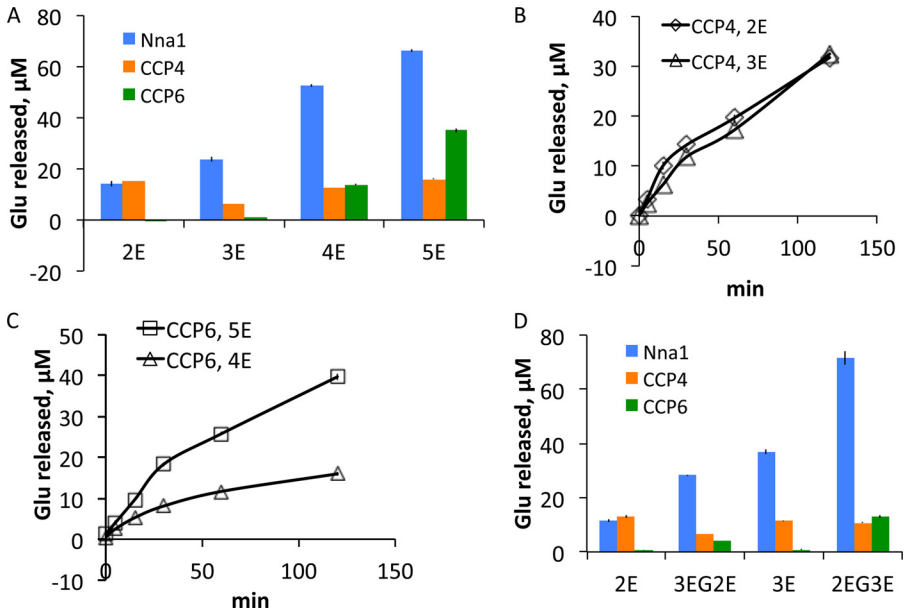

FIGURE 2. **Nna1 family members exhibit different preferences for glutamate chain length.** *A*, using synthetic substrates with increasing glutamate chain length (biotin-2E to biotin-5E) revealed that Nna1 and CCP6 were more active against longer chains, whereas CCP4 showed relatively little preference. Notably, CCP6 did not metabolize substrates with fewer than four glutamate residues. *B*, time course of glutamate release from biotin-2E and biotin-3E with recombinant CCP4 reveals a slight preference for the shorter chain substrate. *C*, time course of glutamate release from biotin-4E and biotin-5E with recombinant CCP6 reveals higher activity for biotin-5E compared with biotin-4E. *D*, influence of neighboring glutamic acids on enzymatic activity. Nna1 and CCP6 activities were enhanced by adjacent glutamic acids, whereas CCP4 was not affected. In all assays, 3 μg of each enzyme was incubated with 40 μM substrate at 37 °C for 1 h, and activity was determined by the amount of glutamate released. *Error bars* are the mean ± S.E. of triplicate determinations.

CCP6 could not metabolize biotin-2E or biotin-3E, it showed significant activity against biotin-3EG2E and biotin-2EG3E (Fig. 2*D*).

Michaelis-Menten analysis was performed to assess what effect glutamate chain length and neighboring amino acid composition have on the kinetic properties of the three enzymes (Table 1). As shown previously for Nna1 (7), increasing the chain length from two to three glutamate residues markedly increased V_{max} (~7-fold increase) with little effect on K_m. In contrast, increasing the glutamate chain length dramatically

TABLE 1
Kinetic parameters of CCPs with different substrates

	Nna1				CCP4				CCP6			
	K_m	V_{max}	k_{cat}	k_{cat}/K_m	K_m	V_{max}	k_{cat}	k_{cat}/K_m	K_m	V_{max}	k_{cat}	k_{cat}/K_m
	μM	*nmol/min*	min^{-1}	$\mu M^{-1}\ s^{-1}$	μM	*nmol/min*	min^{-1}	$\mu M^{-1}\ s^{-1}$	μM	*nmol/min*	min^{-1}	$\mu M^{-1}\ s^{-1}$
Biotin-2E	150	0.79	36.9	0.25	1563	4.59	183.6	0.12	NA[a]	NA	NA	NA
Biotin-3EG2E	74	2.03	94.7	1.28	182	0.53	21.2	0.12	49.4	0.28	5.72	0.12
Biotin-3E	180	5.52	257.6	1.43	299	0.91	36.4	0.12	NA	NA	NA	NA
Biotin-2EG3E	76	4.18	195.1	2.57	94.5	0.5	20	0.21	99.8	0.98	20.02	0.20

[a] NA, not applicable.

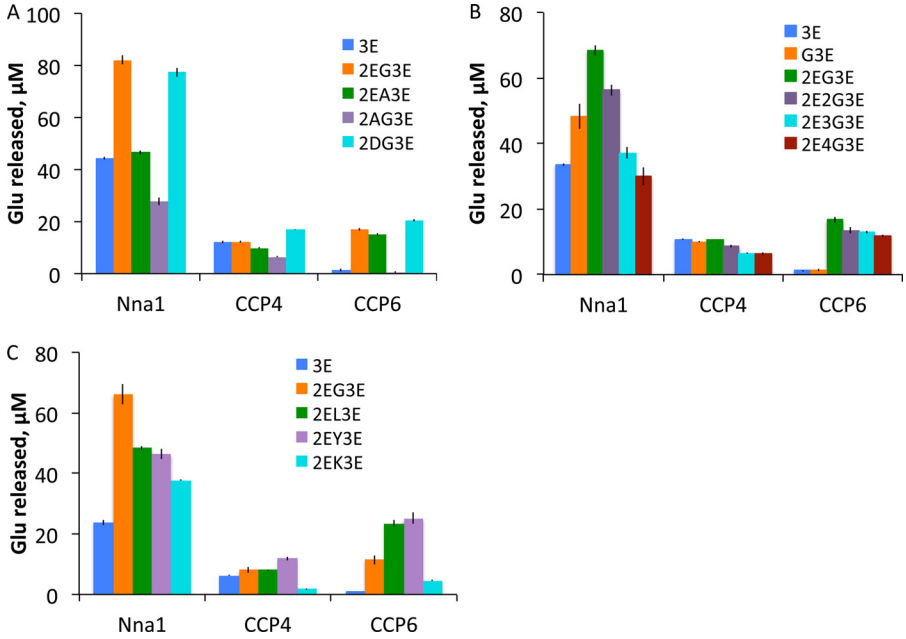

FIGURE 3. **Glutamase activity of Nna1 family members is influenced by amino acids neighboring the polyglutamate chain in the substrate.** *A*, the presence of adjacent glutamic and aspartic acid residues (represented by the substrates biotin-2EG3E and biotin-2DG3E, respectively) enhanced the activities of Nna1 and CCP6, but not CCP4. Substitution of alanine in the same positions (biotin-2AG3E) failed to enhance activity, indicating that negatively charged residues promote higher glutamase activities. Substitution of glycine with alanine at position −4 (biotin-2EA3E) reduced the activity of Nna1, but not CCP4 or CCP6. *B*, influence of spacing between the glutamate chain and adjacent negatively charged amino acids on enzymatic activity. A sequential increase in the spacing between the C-terminal polyglutamate and adjacent glutamic acids with glycine residues resulted in a parallel decline in Nna1 activity. CCP4 and CCP6 were much less affected by increased spacing. *C*, amino acid preference at position −4 in the substrate. Substitution of glycine with leucine, tyrosine, or lysine in biotin-2EG3E resulted in reduced metabolism by Nna1, emphasizing its preference for glycine. In contrast, CCP6 showed a preference for hydrophobic residues, and CCP4 had no preference. The lysine substituent (biotin-2EK3E) dramatically reduced or even abolished the activities of Nna1, CCP4, and CCP6.

reduced the K_m of CCP4 (~5-fold reduction), but in addition, it decreased V_{max} by approximately the same magnitude. Thus, increased glutamate chain length resulted in increased affinity of CCP4 for substrate, but this was achieved at the cost of reduced velocity. As CCP6 did not cleave biotin-2E or biotin-3E, we could not perform kinetic analysis. However, using substrates with flanking acidic amino acids (biotin-3EG2E and biotin-2EG3E) revealed that increasing the chain length from two to three glutamate residues increased V_{max} by ~3-fold as in Nna1, although it also approximately doubled K_m (Table 1).

The presence of flanking acidic amino acids had marked effects on the kinetic properties of all three enzymes (Table 1). Comparing biotin-2E with biotin-3EG2E, the presence of the flanking acidic residues decreased the K_m values of both Nna1 (150 *versus* 74 mM) and CCP4 (1593 *versus* 182 mM), whereas it increased V_{max} of Nna1 and decreased it dramatically for CCP4 (Table 1). Thus, the presence of flanking residues mimicked the effect of increased glutamate chain length for both enzymes. The presence of these residues had a profound effect on CCP6, as the enzyme was essentially inactive on biotin-2E and biotin-3E, but was as active as CCP4 when the acidic residues were present (Fig. 2*D* and Table 1).

These studies provide additional support for the analyses using tubulin as substrate, where Nna1 appeared to be the most active of the three enzymes (Fig. 1*B*). Irrespective of the synthetic substrate tested, k_{cat}/K_m for Nna1 was generally ~10-fold greater than that for CCP4 or CCP6, with the exception of biotin-2E, where it was only twice as efficient as CCP4. The k_{cat}/K_m values for CCP4 and CCP6 were essentially identical for substrates that both could metabolize (Table 1), again supporting time course data using tubulin as substrate (Fig. 1*B*).

We next investigated the specificity of the flanking amino acids. As shown previously, both Nna1 and CCP6, but not CCP4, showed enhanced activity for biotin-2EG3E compared with biotin-3E (Fig. 3*A*). Changing the glycine at position −4 to alanine reduced the activity of Nna1, but had minimal effects on CCP4 and CCP6. Changing the two glutamates at positions −5 and −6 to alanine greatly reduced Nna1 activity and eliminated all CCP6 activity, but only marginally reduced CCP4 activity (Fig. 3*A*). Substitution of the glutamates at positions −5 and −6

with aspartic acid increased the activity of all three enzymes compared with biotin-3E to a similar extent (Fig. 3*A*). Thus, negative charge at positions −5 and −6 is required for enhanced enzymatic activity of all three enzymes.

We next assessed whether the location of the negatively charged amino acids is critical by introducing increasing numbers of glycine residues between the charged amino acids and the cleavable glutamate residues (Fig. 3*B*). Nna1 showed enhanced activity for biotin-G3E compared with biotin-3E, whereas the presence of glycine had little effect on CCP4 and CCP6, underscoring that glycine at this position is important for Nna1. The addition of two glutamate residues to the substrate (biotin-2EG3E) further enhanced the activity of Nna1 and CCP6, but not that of CCP4. Sequential increases in the number of glycine residues resulted in a parallel decline in activity with Nna1, such that three or four glycine residues reduced activity to that observed with biotin-3E (Fig. 3*B*). Although CCP6 activity was greatly enhanced by the presence of flanking glutamate residues, it did not exhibit the same dependence on the spacing of the residues as seen with Nna1 (Fig. 3*B*).

As substitution of alanine for glycine reduced substrate catabolism by Nna1, we examined additional substitutions at this position (Fig. 3*C*). Substrates in which the glycine in biotin-2EG3E was substituted with leucine, tyrosine, or lysine all showed reduced metabolism by Nna1, emphasizing the importance of glycine for Nna1. The lysine substituent was the poorest substrate for Nna1 and also exhibited dramatically reduced metabolism by CCP4 and CCP6 (Fig. 3*C*), suggesting that basic charge juxtaposed to the glutamate chain is generally deleterious to the catalytic activity of these enzymes. Noticeably, whereas leucine and tyrosine substitutions were poorer substrates for Nna1, they were significantly better substrates for CCP6 compared with the equivalent glycine-containing (Fig. 3*C*) and alanine-containing (Fig. 3*A*) substrates. Thus, hydrophobic residues juxtaposed to the glutamate chain enhance the activity of CCP6, a property that distinguishes it from Nna1.

In designing the synthetic substrates, we recognized that one of them (biotin-3EG2E) mimicked the processed C terminus of tubulin. α-Tubulins are unusual in that there is dynamic turnover of their C-terminal tyrosine, which is sequentially removed by a currently unknown enzyme and subsequently re-added by the ATP-dependent enzyme tubulin-tyrosine ligase (26). Biotin-3EG2E represents the C terminus of detyrosinated α-tubulin. Notably, all three Nna1 family members metabolized the terminal glutamate of this substrate (Fig. 4*A*). Thus, we predicted that Nna1 and related enzymes not only trim the polyglutamate chain of tubulin, but also remove the C-terminal glutamate from detyrosinated α-tubulin. To confirm and extend this finding, we synthesized longer biotin-based polypeptides that represented additional C-terminal processed forms of α-tubulin (ΔY, Δ2, and Δ3) (Fig. 4*A*). The ΔY peptide is an elongated form of biotin-3EG2E and was as good a substrate for all three family members (Fig. 4*A*). The Δ2 peptide is a naturally occurring C-terminal truncation of α-tubulin that lacks the terminal EY, and the Δ3 peptide lacks EEY (22, 27). Whereas none of the enzymes significantly metabolized the Δ3 substrate, Nna1 removed the terminal glutamate from the Δ2 substrate. As these enzymes were thought to metabolize only polyglutamate substrates, we performed mass spectrometric analysis of the metabolites produced by digestion of biotin-3EG2E to confirm these findings (Fig. 4*B* and data not shown). Within 15 min, Nna1 metabolized the majority of biotin-3EG2E to biotin-3EGE as well as a small amount of biotin-3EG. By 2 h, almost all of biotin-3EG2E was degraded to biotin-3EGE and large amounts of biotin-3EG (Fig. 4*B*). Both CCP4 and CCP6 metabolized some biotin-3EG2E to biotin-3EGE within 15 min. However, no biotin-3EG was detected at any time point with either enzyme (data not shown), and thus, we were unable to confirm that they possessed a monoglutamase activity like Nna1. In addition, we tested one synthetic substrate (biotin-3EGDE) that was metabolized by Nna1 and also by CCP6 and to a lesser extent by CCP4 (Fig. 4*A*), indicating that the monoglutamase activity of these enzymes may depend on the identity of the preceding amino acid. Such a finding has implications for potential *in vivo* substrates for these enzymes. Nevertheless, only Nna1 could efficiently cleave a single C-terminal glutamate from a tubulin-mimetic substrate, making it a candidate for the enzyme that generates Δ3 tubulin *in vivo*.

CCP4 and CCP6 Fail to Fully Rescue the pcd Phenotype in Vivo—As all three Nna1 family members degraded the polyglutamate chain of tubulin *in vitro*, we assessed whether they are biologically equivalent *in vivo*. Previously, we targeted expression of Nna1, as well as an array of mutant forms of the enzyme, to Purkinje cells of transgenic mice (3, 7) using the cerebellar Purkinje cell-specific *L7*/*pcp2* promoter (12). When the transgenic mice were bred onto a homozygous pcd^{3J} background, *Nna1* (but not catalytically dead mutants) completely rescued Purkinje cell loss and the associated locomotor deficits (3, 7). Using the same strategy, we constructed *L7-CCP4* and *L7-CCP6* transgenes (Fig. 5*A*) and generated multiple independent founder lines of transgenic mice (Fig. 5, *B* and *C*). The lines with the highest levels of mRNA for the fusion transgene (Fig. 5, *B* and *C*, *red boxes*) were selected for investigation and subsequently crossed onto a homozygous pcd^{3J} background.

When visually assessed between 6 and 7 weeks of age, all mice homozygous for the pcd^{3J} allele and harboring any of the *CCP4* or *CCP6* transgenic alleles investigated were ataxic, whereas those harboring a wild-type *Nna1* transgenic allele were indistinguishable from wild-type mice. To quantify locomotor performance, we ran selected strains of transgenic mice on an accelerating rotarod (Fig. 5*C*). pcd^{3J} mice had markedly impaired performance compared with wild-type mice, but expression of Nna1 rescued performance in pcd^{3J} mice (Fig. 5*C*). However, transgenic expression of either CCP4 (lines Tg1 and Tg2) or CCP6 (line Tg8) failed to improve locomotor scores in pcd^{3J} mice (Fig. 5*D*). Therefore, unlike Nna1, neither CCP4 nor CCP6 rescued this functional deficit in pcd^{3J} mice and confirmed the visual observation.

Subsequent to behavioral evaluation, mice were killed, and cerebellar Purkinje cell survival was determined using calbindin-D28K immunohistochemistry (Fig. 6), a marker for Purkinje neurons (28). Representative sections through the cerebellums of 8-week-old wild-type and pcd^{3J} mice and pcd^{3J} mice harboring an *L7-Nna1* transgene revealed a near absence of

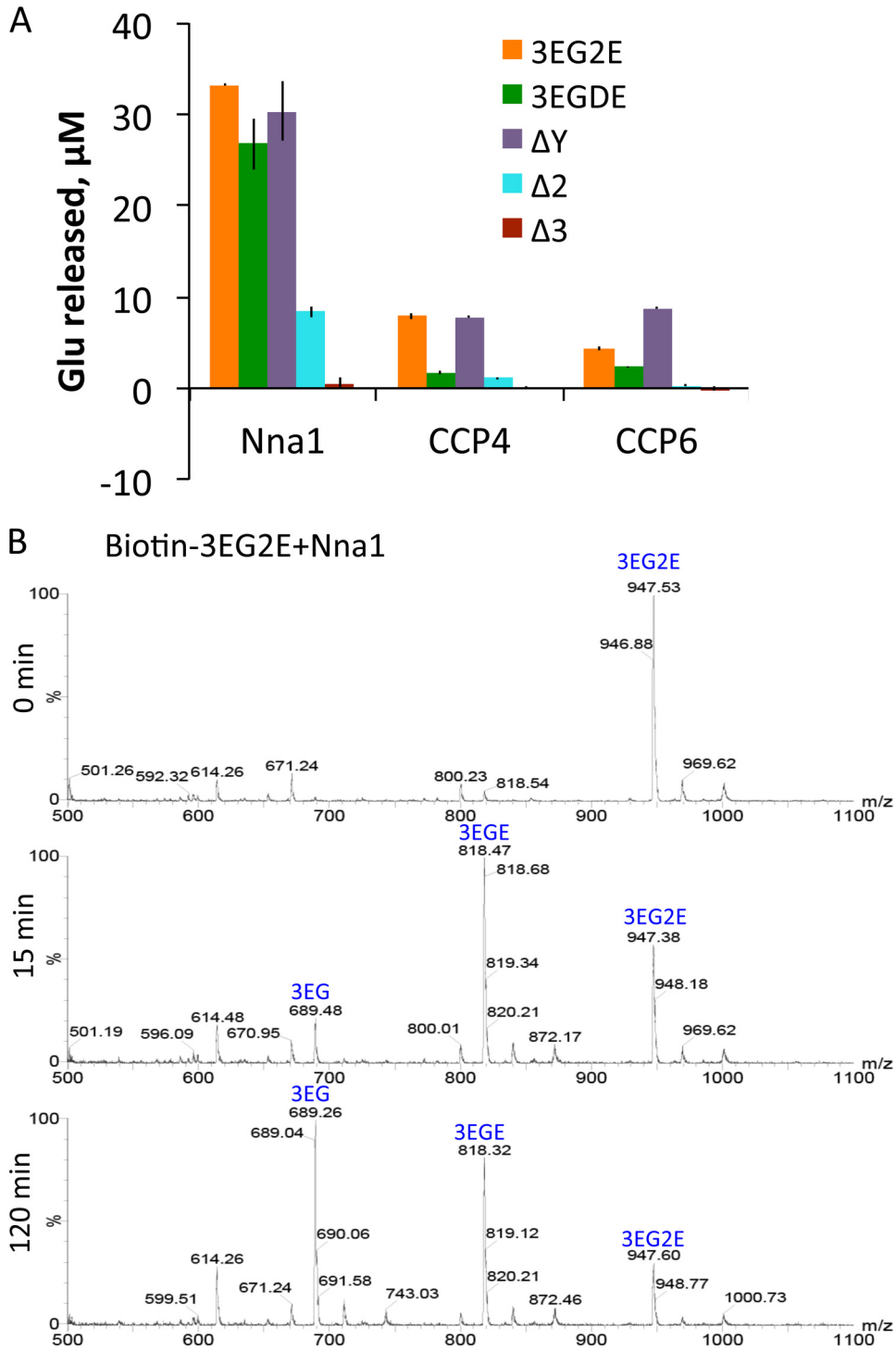

FIGURE 4. **Nna1 family members differentially metabolize synthetic substrates mimicking the C terminus of α-tubulin.** *A*, the activities of Nna1, CCP4, and CCP6 for biotin-based synthetic substrates mimicking the C terminus of α-tubulin. The C terminus of α-tubulin undergoes multiple forms of post-translational modification and processing, including removal and addition of the C-terminal tyrosine and cleavage of glutamate residues at positions −1 and −2 to yield the Δ2 and Δ3 forms, respectively. ΔY (biotin-GEGEEEGEE) mimics the C terminus of detyrosinated α-tubulin, Δ2 (biotin-GEGEEEGE) mimics the Δ2 form of α-tubulin, and Δ3 (biotin-GEGEEEG) mimics the Δ3 form of α-tubulin (22). Nna1 and CCP4 had similar activities for biotin-3EG2E and ΔY, whereas CCP6 favored ΔY over biotin-3EG2E. Nna1 also exhibited activity for Δ2, whereas CCP4 and CCP6 were inactive. None of the enzymes metabolized the Δ3 substrate. These data suggest that Nna1 can generate Δ3 from Δ2. To confirm this, mass spectrometry was employed. *B*, mass spectrometric characterization of metabolites generated from biotin-3EG2E by Nna1. Masses corresponding to biotin-3EG2E, biotin-3EGE, and biotin-3EG are indicated. Within 15 min, Nna1 converted a substantial fraction of biotin-3EG2E to biotin-3EGE, and biotin-3EG was also detectable. By 120 min, substantial amounts of biotin-3EGE and biotin-3EG were produced, accompanied by a dramatic reduction in biotin-3EG2E.

calbindin-D28K-positive neurons in the *pcd*^{3J} mice that was largely rescued by an *L7-Nna1* transgene (Fig. 6, *A*–*C*). Cerebellums from three lines of *pcd*^{3J}/*L7-CCP4* mice and two lines of *pcd*^{3J}/*L7-CCP6* mice showed a large deficit in Purkinje cell numbers, although some Purkinje cells survived, particularly in the posterior cerebellum (Fig. 6, *D*–*H*). The highest rescue was

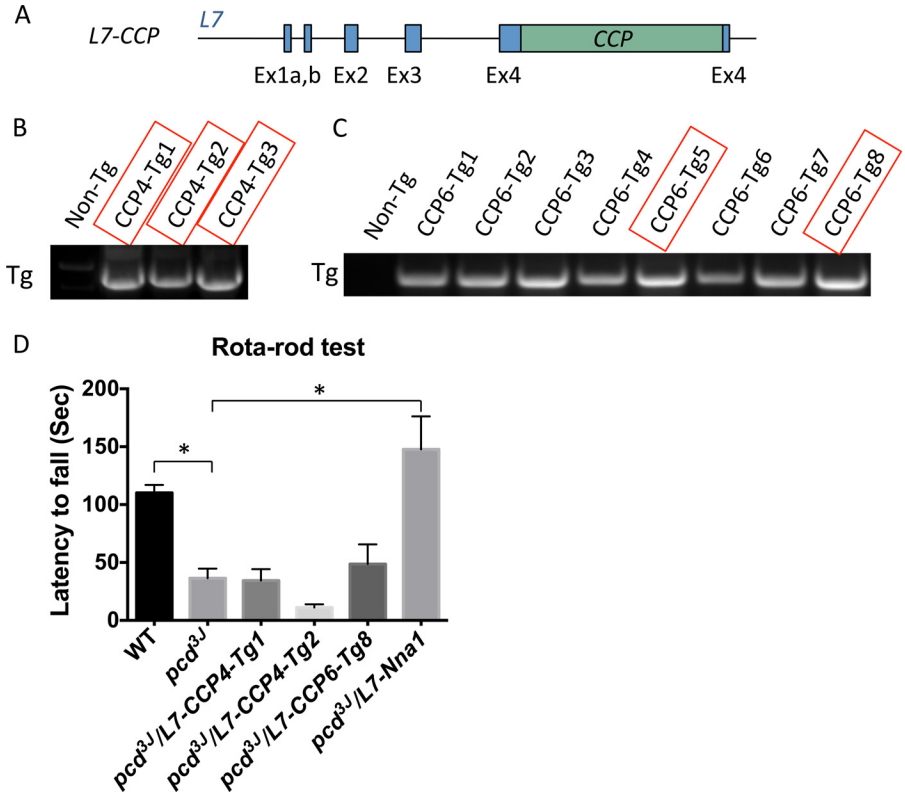

FIGURE 5. ***CCP4* and *CCP6* fail to rescue ataxia in *pcd* mice.** *A*, schematic representation of *L7-CCP* transgenes. The respective *CCP* cDNA was inserted into a unique BamHI site in the fourth exon (*Ex*) of the *L7* gene. *B* and *C*, representative RT-PCR amplification of chimeric transgenic mRNA from total RNA from the cerebellums of wild-type (non-transgenic (*non-Tg*)) and different *L7-CCP4* (*B*) and *L7-CCP6* (*C*) transgenic lines. For each transgene, the lines chosen for further investigation are *boxed* in *red*. *D*, gender-balanced littermates of each genotype ($n = 6–8$/genotype) at 2 months of age were tested on a standardized accelerating rotarod. Wild-type and $pcd^{3J-/-}$ mice and $pcd^{3J-/-}$ mice harboring the *L7-CCP4* (lines Tg1 and Tg2), *L7-CCP6* (line Tg8), or *L7-Nna1* transgene were tested for 5 consecutive days. The latency to fall (in seconds) for all animals of a given genotype was recorded and is presented as the mean ± S.E., but for brevity and clarity, we present only day 1 values. One-way analysis of variance showed that only the wild-type and $pcd^{3J-/-}$/*L7-Nna1* groups differed significantly (*, $p < 0.05$) from the $pcd^{3J-/-}$ group. Therefore, in contrast to Nna1, neither CCP4 nor CCP6 improved locomotor scores in $pcd^{3J-/-}$ mice.

observed for the Tg1 line of *L7-CCP4* mice and the Tg5 line of *L7-CCP6* transgenic mice, and these two strains were selected for further evaluation.

Purkinje cell loss in *pcd* mice is progressive and occurs over a 2–3-month period starting at around day 18 after birth, with Purkinje cells in lobule X being the last to degenerate (29). Therefore, we examined the *L7-CCP4* (Tg1) and *L7-CCP6* (Tg5) lines at 4 months of age. Compared with 2 months of age, fewer Purkinje cells remained in pcd^{3J}/*L7-CCP4* and pcd^{3J}/*L7-CCP6* mice, with the *CCP6* gene seeming to provide a slightly better rescue than the *CCP4* transgenic allele (Fig. 6, *I* and *J*). Together, these data suggest that CCP4 and CCP6 slow but cannot prevent Purkinje cell degeneration in some areas of the cerebellum and that this limited preservation of neurons is insufficient to prevent ataxia.

DISCUSSION

Nna1 is broadly expressed in the developing and adult nervous system, as well as other tissues and organs, yet the pathology in *pcd* mice involves only a few defined populations of neurons in adult brain and spermatogenesis in the testis (4, 29). To explain this observation, we hypothesized that Nna1-related enzymes might compensate for loss of Nna1 function in unaffected neurons and tissues. For this to be true, we would anticipate that the related enzymes should not only have similar enzymatic properties to Nna1, but should also be able to rescue Nna1 deficiency *in vivo*. Therefore, we examined the enzymatic and biological properties of CCP4, a glutamase whose overall architecture and amino acid sequence homology are most like Nna1, as well as CCP6, one of the most divergent family members (2, 3), whose expression is low in the cerebellum but relatively high in other brain areas (2, 10). We showed that although Nna1, CCP4, and CCP6 all removed glutamate from the polyglutamate chain of tubulin *in vitro* (Fig. 1, *B* and *C*), they had different kinetic properties (Fig. 1 and Table 1) and substrate specificities (Figs. 2–4) and that neither CCP4 nor CCP6 fully substituted for Nna1 in cerebellar Purkinje cells *in vivo* (Figs. 5 and 6).

Both the *L7-CCP4* and *L7-CCP6* transgenes expressed relatively high levels of their respective mRNAs, which were confined to Purkinje cells and exceeded the endogenous mRNA levels of these two enzymes in the whole cerebellum and whole cerebral cortex in adult mice (Fig. 5, *B* and *C*; and data not shown) (2, 3, 10). Indeed, endogenous *CCP4* mRNA is almost undetectable in the adult cerebellum (2, 3, 10), and levels of *CCP6* mRNA are low in the cerebellum but much higher in other brain regions (2, 10), making it a good candidate to explain the selectivity of cell death in *pcd* mice. However, the lack of efficacy of CCP4 or CCP6 *in vivo* suggests that the selec-

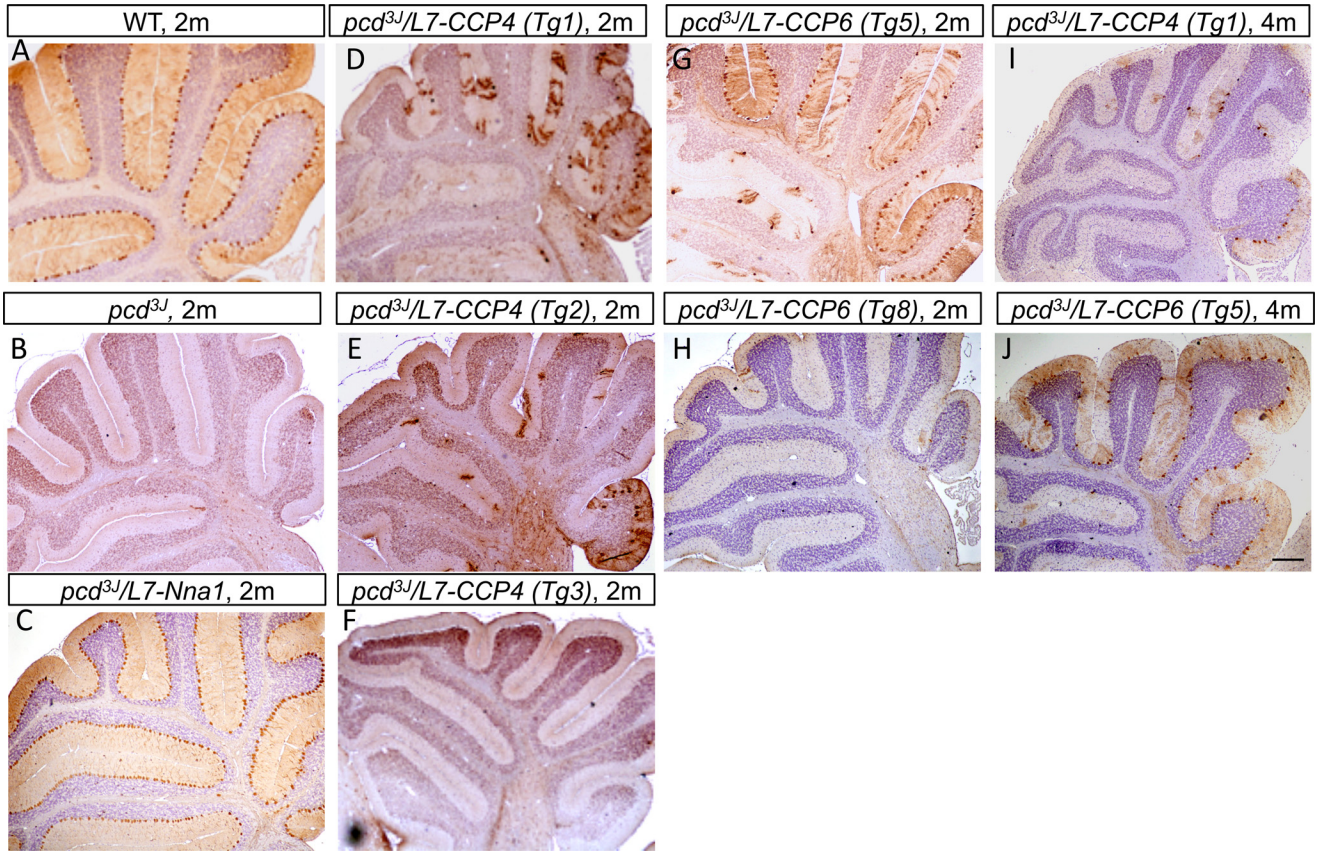

FIGURE 6. ***CCP4* and *CCP6* fail to fully rescue Purkinje cell death in *pcd* mice.** Shown are calbindin-D28K immunohistochemistry and hematoxylin counterstaining of cerebellar sections from 2-month-old (*2m*; *A–H*) and 4-month-old (*4m*; *I* and *J*) wild-type mice (*A*), $pcd^{3J-/-}$ mice (*B*), $pcd^{3J-/-}$ mice harboring the *L7-Nna1* transgene (*C*), $pcd^{3J-/-}$ mice harboring three independent alleles (Tg1, Tg2, and Tg3) of the *L7-CCP4* transgene (*D–F* and *I*), and $pcd^{3J-/-}$ mice harboring two independent alleles (Tg5 and Tg8) of the *L7-CCP6* transgene (*G*, *H*, and *J*). Note at 2 months the loss of calbindin-positive Purkinje neurons in $pcd^{3J-/-}$ mice (*B*), whereas the *L7-Nna1* transgene prevented Purkinje neuron loss (*C*). In contrast, cerebellums from each line of $pcd^{3J-/-}$/*L7-CCP4* (*D–F*) and $pcd^{3J-/-}$/*L7-CCP6* (*G* and *H*) mice showed a large deficit in Purkinje cell numbers, although some Purkinje cells (predominantly in the posterior cerebellum) survived (*e.g. L7-CCP4-Tg1* and *Tg2* (*D* and *E*) and *L7-CCP6-Tg5* (*G*)). At 4 months of age, Purkinje cell numbers in the cerebellums of $pcd^{3J-/-}$/*L7-CCP4-Tg1* (*I*) and $pcd^{3J-/-}$/*L7-CCP6-Tg5* (*J*) mice were further reduced compared with those from 2-month-old animals (*D* and *G*, respectively). Therefore, CCP4 and CCP6 appear to slow but not prevent Purkinje cell death and cannot replace the function of Nna1 *in vivo*. *Scale bar* = 200 μm.

tive neuropathology in *pcd* mice is not attributable to functional compensation by *CCP4* or *CCP6* in unaffected neuronal populations. However, formal proof of this will require eliminating CCP6 expression in resistant neurons in the context of a *pcd* mouse. Whether other Nna1 family members fulfill this role also remains to be established. It is also remarkable that transgenic overexpression of *Nna1*, *CCP4*, and *CCP6* in Purkinje cells did not trigger any overt anomalies in otherwise wild-type mice. This suggests that a shift toward longer polyglutamate chains in Purkinje cells of *pcd* mice is deleterious, whereas a shift toward shorter chains in Purkinje cells of *CCP* gain-of-function mice is innocuous. If true, it would be interesting to assess the ratio of anabolic TTLL enzymatic activities to catabolic CCP activities in sensitive and resistant neuronal populations. Potentially, unaffected neurons might have low TTLL activity and shorter polyglutamate chains compared with susceptible populations and so could more readily compensate for or tolerate loss of individual CCPs.

This study raises the question of why *CCP4* and *CCP6* fail to completely rescue the *Nna1*-null phenotype when both are capable of metabolizing the polyglutamate chain of tubulin. Potential explanations include the relative catalytic efficiency of each enzyme on polyglutamylated tubulin, the relative stability of CCPs in Purkinje cells, their interaction with or requirement for other proteins or molecules in Purkinje cells, and even that tubulin is not the substrate underlying the toxicity. *In vitro*, Nna1 is the most efficient of the three enzymes with both tubulin and synthetic tubulin mimetics as substrates. k_{cat}/K_m for Nna1 is ~10 times that for CCP4 and CCP6 with two relevant tubulin-mimetic substrates (Table 1). Therefore, although small amounts of *Nna1* mRNA completely rescue the *pcd* phenotype (3) and the transgenes generate relatively large amounts of *CCP4* and *CCP6* mRNAs compared with endogenous levels of their mRNAs, this may still be insufficient to prevent Purkinje cell death. The delayed progression of degeneration in the *L7-CCP4* and *L7-CCP6* mice may be a reflection of a situation in which the process is slowed but not prevented.

The delay of Purkinje cell death caused by *CCP4* and *CCP6* expression in *pcd* mice was notably more pronounced in the posterior regions of the cerebellum (Fig. 6). Purkinje cell loss in *pcd* mice is progressive: beginning in the third week after birth, Purkinje cell death increases rapidly over the ensuing 2 weeks, along with the emergence of ataxia, and is largely complete by 2 months of age (29). However, some Purkinje cells in the posterior cerebellum, notably lobule X, survive longer, although by 4 months, essentially all Purkinje cells have degenerated (29). The

basis of this temporally and anatomically graded degeneration is not known. It is possible that Purkinje cells in the anterior and posterior cerebellum have different expression profiles of TTLL enzymes and CCPs that enable posterior Purkinje cells to survive longer in the absence of Nna1 and even longer when supplemented with either CCP4 or CCP6. However, a similar anatomical pattern of degeneration is seen in the woozy mouse, which has a homozygous disruption of the BiP co-chaperone SIL1 (30). As the underlying mutations in *pcd* and woozy mice ostensibly affect different cellular processes, it may be that Purkinje cells in the posterior regions of the cerebellum express genes that render them generally more resistant to degeneration, rather than there being differences in expression of TTLL enzymes and CCPs.

The present data are also relevant to broader aspects of post-translational processing of tubulin. The C-terminal regions of tubulins undergo multiple forms of post-translational modifications, which, in addition to polyglutamylation, include removal and addition of a C-terminal tyrosine residue, addition and trimming of polyglycine side chains, and proteolytic processing to yield Δ2 tubulin (reviewed in Ref. 31). Nna1 appears to be involved in several of these processes, as it not only removes polyglutamate chains from tubulin (Fig. 1, *B* and *C*) (7, 10, 22), but also cleaves synthetic substrates that mimic the detyrosinated and Δ2 forms of the C terminus of α-tubulin (Fig. 4*A*). Furthermore, as tubulin-tyrosine ligase requires two glutamate residues in the substrate for activity (26), metabolism of detyrosinated tubulin by Nna1 family members will preclude further tyrosination and lead to the accumulation of Δ2 tubulin. By extension, this also suggests that the tyrosinated form of tubulin would be elevated in *pcd* mice. This raises the question of whether elevated tyrosinated tubulin levels contribute to the *pcd* phenotype. Our data also indicate that Nna1, but not CCP4 or CCP6, efficiently cleaves the glutamate from a Δ2 tubulin-mimetic substrate, suggesting that it may also be responsible for the further degradation of tubulin *in vivo*.

Polyglutamylation has been confirmed only by structural analysis on tubulins and nucleosome assembly proteins (24, 25, 32), and so our data also provide evidence for potential additional substrates for the Nna1 family of proteins. Janke and co-workers (33) performed the most extensive analysis of polyglutamylation sites in proteins, and although no absolute consensus sequence emerged, glutamylation (and glycylation) took place on a γ-carboxyl group of a glutamic acid in a glutamate-rich region of the protein. As polyglutamylation is a dynamic process in which glutamate residues are both added and removed, it is unclear whether the presence of glutamate-rich sequences is required for the anabolic, catabolic, or both aspects of chain metabolism. Our data indicate that the presence of nearby glutamate residues enhances the efficacy of the Nna1 family of glutamases. In addition, aspartic acid can fulfill this role, although we do not know whether it can substitute for glutamate residues in terms of chain initiation and elongation. Regardless, our data support the notion that nearby aspartic acid residues can enhance enzymatic activity against C-terminal glutamate residues. Moreover, although none of the enzymes metabolized polyaspartate (data not shown), a penultimate aspartate residue conferred a monoglutamase activity on all three CCP family members (Fig. 4*A*). These findings potentially expand the range of *in vivo* substrates and products for the Nna1 family of enzymes.

Although all three Nna1 family members have glutamase activities and remove the polyglutamate chains of tubulin, our data establish that they can be distinguished on the basis of their kinetic properties and substrate preferences. Nna1 is the most active enzyme against tubulin and synthetic substrates with longer glutamate chains, and nearby acidic residues further enhance its activity. Thus, not only is k_{cat}/K_m for Nna1 ~10 times higher than for the other CCPs examined for a given substrate, it also increases with increasing glutamate chain length, and the presence of flanking acidic residues increases k_{cat}/K_m for a given glutamate chain length. This is achieved by increases in V_{max} with relatively small effects on K_m. In contrast, CCP4 has little preference for glutamate chain length or the presence of flanking acidic residues. However, both parameters do influence K_m and V_{max}, but in a reciprocal fashion. Thus, increasing the glutamate chain length markedly decreases K_m, as does the presence of flanking glutamate residues. However, this gain in affinity results in a large decrease in V_{max}, such that there is little change in overall metabolism. One point of note is that at high concentrations of short chain substrates, CCP4 is predicted to be more active than Nna1. Additional distinctions exist in substrate preference between Nna1 and CCP4. For example, Nna1 favors a glycine juxtaposed to the glutamate chain, whereas CCP4 has little preference for amino acid identity at this position and generally behaves as a promiscuous glutamase. The marked difference in kinetics between Nna1 and CCP4 was not anticipated, as they are structurally very similar and have relatively high levels of sequence homology in both their catalytic domains and their long N-terminal regions, the function of which is not known (2, 3). Despite being structurally dissimilar to Nna1 and CCP4, the catalytic properties of CCP6 were intermediate between these two enzymes. Unlike CCP4, CCP6 is highly dependent upon flanking acidic amino acids and, in their absence, will metabolize substrates only with more than three glutamate residues. Like Nna1, this is attributable to an increase in V_{max}, with longer glutamate chains associated with a slight loss of affinity. However, in contrast to Nna1, CCP6 favors a hydrophobic amino acid juxtaposed to the glutamate chain. A common feature of all three enzymes is that lysine adjacent to the glutamate chain reduces enzymatic activity and emphasizes that acidic substrates are preferred. Taken together, these data suggest that the three CCPs metabolize both common and distinct substrates, and their relative contributions to the deglutamylation of common substrates will depend on both amino acid sequence and substrate concentration.

Acknowledgments—We thank Qun Liu (Department of Developmental Neurobiology, St. Jude Children's Research Hospital) for technical assistance and the Hartwell Center for Bioinformatics and Biotechnology and the Protein Production Facility of St. Jude Children's Research Hospital for assistance with substrate synthesis and protein purification, respectively. We also thank Dr. R. Kiplin Guy (Department of Chemical Biology and Therapeutics, St. Jude Children's Research Hospital) for advice and critical evaluation of the manuscript.

REFERENCES

1. Harris, A., Morgan, J. I., Pecot, M., Soumare, A., Osborne, A., and Soares, H. D. (2000) Regenerating motor neurons express Nna1, a novel ATP/GTP-binding protein related to zinc carboxypeptidases. *Mol. Cell. Neurosci.* **16,** 578–596
2. Kalinina, E., Biswas, R., Berezniuk, I., Hermoso, A., Aviles, F. X., and Fricker, L. D. (2007) A novel subfamily of mouse cytosolic carboxypeptidases. *FASEB J.* **21,** 836–850
3. Wang, T., Parris, J., Li, L., and Morgan, J. I. (2006) The carboxypeptidase-like substrate-binding site in Nna1 is essential for the rescue of the Purkinje cell degeneration (*pcd*) phenotype. *Mol. Cell. Neurosci.* **33,** 200–213
4. Fernandez-Gonzalez, A., La Spada, A. R., Treadaway, J., Higdon, J. C., Harris, B. S., Sidman, R. L., Morgan, J. I., and Zuo, J. (2002) Purkinje cell degeneration (*pcd*) phenotypes caused by mutations in the axotomy-induced gene, *Nna1*. *Science* **295,** 1904–1906
5. Wang, T., and Morgan, J. I. (2007) The Purkinje cell degeneration (*pcd*) mouse: an unexpected molecular link between neuronal degeneration and regeneration. *Brain Res.* **1140,** 26–40
6. Zhao, X., Onteru, S. K., Dittmer, K. E., Parton, K., Blair, H. T., Rothschild, M. F., and Garrick, D. J. (2012) A missense mutation in *AGTPBP1* was identified in sheep with a lower motor neuron disease. *Heredity* **109,** 156–162
7. Wu, H. Y., Wang, T., Li, L., Correia, K., and Morgan, J. I. (2012) A structural and functional analysis of Nna1 in Purkinje cell degeneration (*pcd*) mice. *FASEB J.* **26,** 4468–4480
8. Chakrabarti, L., Eng, J., Martinez, R. A., Jackson, S., Huang, J., Possin, D. E., Sopher, B. L., and La Spada, A. R. (2008) The zinc-binding domain of Nna1 is required to prevent retinal photoreceptor loss and cerebellar ataxia in Purkinje cell degeneration (*pcd*) mice. *Vision Res.* **48,** 1999–2005
9. Kimura, Y., Kurabe, N., Ikegami, K., Tsutsumi, K., Konishi, Y., Kaplan, O. I., Kunitomo, H., Iino, Y., Blacque, O. E., and Setou, M. (2010) Identification of tubulin deglutamylase among *Caenorhabditis elegans* and mammalian cytosolic carboxypeptidases (CCPs). *J. Biol. Chem.* **285,** 22936–22941
10. Rogowski, K., van Dijk, J., Magiera, M. M., Bosc, C., Deloulme, J. C., Bosson, A., Peris, L., Gold, N. D., Lacroix, B., Bosch Grau, M., Bec, N., Larroque, C., Desagher, S., Holzer, M., Andrieux, A., Moutin, M. J., and Janke, C. (2010) A family of protein-deglutamylating enzymes associated with neurodegeneration. *Cell* **143,** 564–578
11. Janke, C., Rogowski, K., and van Dijk, J. (2008) Polyglutamylation: a fine-regulator of protein function? 'Protein Modifications: beyond the usual suspects' review series. *EMBO Rep.* **9,** 636–641
12. Oberdick, J., Smeyne, R. J., Mann, J. R., Zackson, S., and Morgan, J. I. (1990) A promoter that drives transgene expression in cerebellar Purkinje and retinal bipolar neurons. *Science* **248,** 223–226
13. Rong, Y., Wang, T., and Morgan, J. I. (2004) Identification of candidate Purkinje cell-specific markers by gene expression profiling in wild-type and *pcd*^{3J} mice. *Brain Res. Mol. Brain Res.* **132,** 128–145
14. Wei, P., Blundon, J. A., Rong, Y., Zakharenko, S. S., and Morgan, J. I. (2011) Impaired locomotor learning and altered cerebellar synaptic plasticity in *pep-19*/*pcp4*-null mice. *Mol. Cell. Biol.* **31,** 2838–2844
15. Doi, E., Shibata, D., and Matoba, T. (1981) Modified colorimetric ninhydrin methods for peptidase assay. *Anal. Biochem.* **118,** 173–184
16. Coombs, T. L., Felber, J. P., and Vallee, B. L. (1962) Metallocarboxypeptidases: mechanism of inhibition by chelating agents, mercaptans, and metal ions. *Biochemistry* **1,** 899–905
17. Vallee, B. L., and Neurath, H. (1955) Carboxypeptidase, a zinc metalloenzyme. *J. Biol. Chem.* **217,** 253–261
18. Mathews, C. K., van Holde, K. E., and Ahern, K. G. (2000) Enzymes: biological catalysis. in *Biochemistry*, 3rd Ed., pp. 375–395, Addison Wesley Longman Publishing Co., San Francisco
19. Buitrago, M. M., Ringer, T., Schulz, J. B., Dichgans, J., and Luft, A. R. (2004) Characterization of motor skill and instrumental learning time scales in a skilled reaching task in rat. *Behav. Brain Res.* **155,** 249–256
20. Gagnon, C., White, D., Cosson, J., Huitorel, P., Eddé, B., Desbruyères, E., Paturle-Lafanechère, L., Multigner, L., Job, D., and Cibert, C. (1996) The polyglutamylated lateral chain of alpha-tubulin plays a key role in flagellar motility. *J. Cell Sci.* **109,** 1545–1553
21. Ikegami, K., Heier, R. L., Taruishi, M., Takagi, H., Mukai, M., Shimma, S., Taira, S., Hatanaka, K., Morone, N., Yao, I., Campbell, P. K., Yuasa, S., Janke, C., Macgregor, G. R., and Setou, M. (2007) Loss of α-tubulin polyglutamylation in ROSA22 mice is associated with abnormal targeting of KIF1A and modulated synaptic function. *Proc. Natl. Acad. Sci. U.S.A.* **104,** 3213–3218
22. Berezniuk, I., Vu, H. T., Lyons, P. J., Sironi, J. J., Xiao, H., Burd, B., Setou, M., Angeletti, R. H., Ikegami, K., and Fricker, L. D. (2012) Cytosolic carboxypeptidase 1 is involved in processing α- and β-tubulin. *J. Biol. Chem.* **287,** 6503–6517
23. Alexander, J. E., Hunt, D. F., Lee, M. K., Shabanowitz, J., Michel, H., Berlin, S. C., MacDonald, T. L., Sundberg, R. J., Rebhun, L. I., and Frankfurter, A. (1991) Characterization of posttranslational modifications in neuron-specific class III beta-tubulin by mass spectrometry. *Proc. Natl. Acad. Sci. U.S.A.* **88,** 4685–4689
24. Eddé, B., Rossier, J., Le Caer, J. P., Promé, J. C., Desbruyères, E., Gros, F., and Denoulet, P. (1992) Polyglutamylated alpha-tubulin can enter the tyrosination/detyrosination cycle. *Biochemistry* **31,** 403–410
25. Redeker, V., Melki, R., Promé, D., Le Caer, J. P., and Rossier, J. (1992) Structure of tubulin C-terminal domain obtained by subtilisin treatment. The major α and β tubulin isotypes from pig brain are glutamylated. *FEBS Lett.* **313,** 185–192
26. Rüdiger, M., Plessman, U., Klöppel, K. D., Wehland, J., and Weber, K. (1992) Class II tubulin, the major brain β tubulin isotype, is polyglutamylated on glutamic acid residue 435. *FEBS Lett.* **308,** 101–105
27. Paturle-Lafanechère, L., Eddé, B., Denoulet, P., Van Dorsselaer, A., Mazarguil, H., Le Caer, J. P., Wehland, J., and Job, D. (1991) Characterization of a major brain tubulin variant which cannot be tyrosinated. *Biochemistry* **30,** 10523–10528
28. Iacopino, A. M., Rhoten, W. B., and Christakos, S. (1990) Calcium binding protein (calbindin-D28k) gene expression in the developing and aging mouse cerebellum. *Brain Res. Mol. Brain Res.* **8,** 283–290
29. Mullen, R. J., Eicher, E. M., and Sidman, R. L. (1976) Purkinje cell degeneration, a new neurological mutation in the mouse. *Proc. Natl. Acad. Sci. U.S.A.* **73,** 208–212
30. Zhao, L., Longo-Guess, C., Harris, B. S., Lee, J. W., and Ackerman, S. L. (2005) Protein accumulation and neurodegeneration in the woozy mutant mouse is caused by disruption of SIL1, a cochaperone of BiP. *Nat. Genet.* **37,** 974–979
31. Fukushima, N., Furuta, D., Hidaka, Y., Moriyama, R., and Tsujiuchi, T. (2009) Post-translational modifications of tubulin in the nervous system. *J. Neurochem.* **109,** 683–693
32. Regnard, C., Desbruyères, E., Huet, J. C., Beauvallet, C., Pernollet, J. C., and Eddé, B. (2000) Polyglutamylation of nucleosome assembly proteins. *J. Biol. Chem.* **275,** 15969–15976
33. van Dijk, J., Miro, J., Strub, J. M., Lacroix, B., van Dorsselaer, A., Eddé, B., and Janke, C. (2008) Polyglutamylation is a post-translational modification with a broad range of substrates. *J. Biol. Chem.* **283,** 3915–3922
34. National Institutes of Health. (1996) *National Institutes of Health guide for the care and use of laboratory animals*, NIH Publication No. 80-23, National Institutes of Health, Bethesda, MD